

# Ground Support Design for Sudden and Violent Failures in Hard Rock Tunnels

E. Villaescusa<sup>a\*</sup> A. Kusui<sup>a</sup> and C. Drover<sup>a</sup>

<sup>a</sup> *Western Australian School of Mines-Curtin University of Technology, CRC Mining, Locked Bag 30, Kalgoorlie, WA, 6430 Australia*

\* [E.Villaescusa@curtin.edu.au](mailto:E.Villaescusa@curtin.edu.au)

## Abstract

The performance of ground support for an excavation under high stress largely depends upon the potential block size associated with any violent ejection. The larger the mobilized blocks, the more reinforcement action that will be involved in dissipating energy. Conversely, small block size instability requires membrane support, such as that provided by combinations of shotcrete, mesh, rockbolt and cablebolt plates. In general, the energy demand from a particular failure is controlled by the amount of mass that becomes unstable and the velocity of its ejection. This paper presents a new methodology in which the ground support demand can be expressed in terms of the maximum mass in tonnes of unstable rock that is ejected per unit area of the excavation surface where failure occurs. The methodology described here considers that the strain energy released by the rock mass during violent stress-driven failure is converted into kinetic energy of the ejected blocks. These blocks load the ground support scheme dynamically, causing a force-displacement response. An acceptable design involves the selection of ground support schemes which have sufficient energy dissipation and displacement capacity to exceed the energy and displacement demand imposed by an ejecting mass. A high energy dissipation ground support strategy for extremely high demand rock mass conditions is also presented.

**Keywords:** Violent failure, Design, Laboratory testing, Field testing, Ground support, Deep excavations, High stress, Damage, Tunnels.

## 1. Introduction

Underground excavations are reaching depths below the ground surface where the ratio of intact rock strength to induced stresses is such that violent failure of the rock mass adjacent to the excavation can occur very soon after construction. Observations and geotechnical monitoring indicate that complex high energy failure mechanisms frequently intersect the excavations. In most cases, the depth of failure is contained within the length of the rock reinforcement elements. For a typical mining or civil tunnelling excavation, this length is commonly 2.5-4.0 m. Where the depth of failure is shallow (<0.5 m), this often involves damage of the surface support, which in some cases does not have the capacity to transfer load to the reinforcement elements (Fig. 1).



Fig. 1. Lack of ground support retention following a violent spalling failure near the surface of an excavation.

In some cases, however, the violent failures mobilise geological structures and the depth of failure can be more significant ( $>1.0$  m), often involving failure through the reinforcement elements. This can occur where large scale geological structures are sub-parallel to the tunnel walls or form wedges that control the shape and depth of failure (Fig. 2). Excavation instabilities having a depth of failure ranging from 0.5 to 1.0 m are considered to be transitional and may involve a mixture of both support and reinforcement mobilization.



Fig. 2. Failure of reinforcement elements following violent, structurally controlled instability.

The load transfer mechanism for an excavation under high stress is very complex and depends upon the level of pre-existing rock mass damage and potential block size associated with violent ejections. The larger the mobilized blocks, the more reinforcement action that will be involved in dissipating energy. Conversely, small block size instability requires membrane support, such as that provided by combinations of shotcrete and mesh. In all cases, the performance of the surface support is critical to

achieve load transfer to the reinforcement elements, which in turn stabilize the excavations (Thompson and Windsor, 1992).

## 2. Tunnel Instability

The ratio of intact rock Uniaxial Compressive Strength ( $\sigma_c$ ) to the induced compressive stress tangential to the wall of an excavation ( $\sigma_{max}$ ) has long been recognized as a critical factor controlling excavation stability (Barton et al., 1974; Mathews et al., 1980). As the ratio of  $\sigma_c/\sigma_{max}$  reduces, excavation instability increases, as shown in Fig. 3. Data from many years of numerical modelling and observations of open stoping in hard rock at Mount Isa Mines (Villaescusa, 2014) have shown that as the ratio decreases below the value of 3, the instability increases markedly. In general, when excavating in rock with  $\sigma_c/\sigma_{max}$  ratios below 5, it can be expected that large deformations would be experienced in tunnels driven within low strength rock, while sudden, violent failure could occur in tunnels excavated in high strength rock (Barla, 2014).

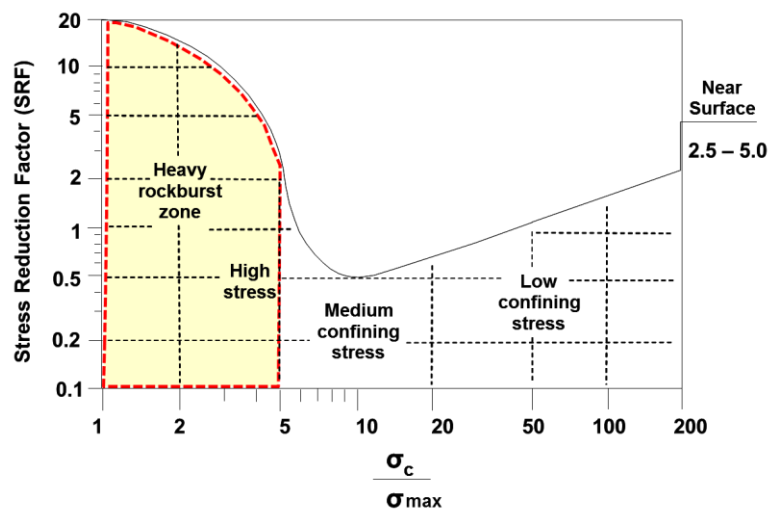


Fig. 3. Excavation behaviour as a function of the ratio of compressive strength to the induced stress. (After Barton et al., 1974; Hutchinson and Diederichs, 1996).

The relationship between the rock strength and the induced stress at the onset of failure has been investigated by a number of researchers using stress-strain data from UCS laboratory testing (Diederichs, 2007; Lajtai & Dzik, 1996; Martin, 1997). The research shows that failure initiates when the ratio of the uniaxial compressive strength obtained by laboratory testing ( $\sigma_c$ ) to the stress magnitude causing the failure ( $\sigma_{max}$ ) ranges between 2 and 3. Martin (1993) also conducted detailed investigations at an underground excavation at the AECL in Canada. The crack propagation process started when the intact strength to induced stress ratio reached approximately 2.

### 2.1 Spalling Failure

Spalling failure of an excavation under high compressive stress is characterised by tensile fracturing of rock in an orientation typically sub-parallel to both the major principal stress component and adjacent excavation surface, often with associated ejection of rock slabs. Spalling fractures may be few, occurring through intact rock, or highly repetitive and closely spaced due to delamination of pre-existing discontinuity surfaces that are suitably oriented. Stress-driven damage in brittle rock often occurs initially as progressive violent spalling of the excavation walls and is localized within areas of maximum induced stress concentrations (Christiansson et al., 2012). Such failures typically result in an approximately v-shaped notch in the regions of violent ejection (Fig. 4).



Fig. 4. Example of notch formation due to brittle failure in an underground tunnel.

Recent laboratory work by Kusui et al (2016) has calculated the ratio of compressive strength to induced stress at the sidewalls of scaled-down tunnels which have been progressively loaded to failure. For the first stage of failure, where spalling was experienced, the ratio monitored was the value of compressive strength to maximum tangential stress (i.e. effectively near zero confining stress at the excavation boundary). A total of 17 unsupported laboratory tests were performed for a range of intact rock strengths, the results of which are shown in Fig. 5. The ratio of  $\sigma_c$  to  $\sigma_{max}$  was calculated using the Kirsch solution and also checked with finite element modelling using the program Abaqus (Kusui et al, 2016). The stress value was calculated for both sides of the tunnel during wall spalling. Similar to previous published work (Martin, 1993), violent ejection from the excavation walls occurred prior to peak intact rock strength. The strength/induced stress ratio at spalling and the uniaxial compressive strength show a strong correlation. The value of  $\sigma_c/\sigma_{max}$  at spalling ranges from 2 to 3.5 for strong to very strong rock. The red dotted line and related equation shown in Fig. 5 represents the potential onset of failure. i.e., what could be interpreted as the practical safe limits prior to spalling failure. The samples of moderately strong rock ( $\sigma_c < 50\text{MPa}$ ) did not fail violently.

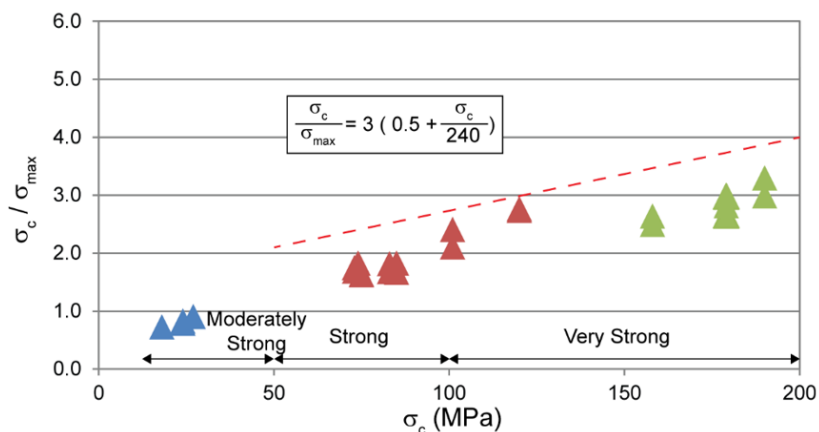


Fig. 5. Unsupported tunnel spalling as a function of compressive strength and maximum tangential stress (Kusui et al, 2016).

The laboratory results from Kusui (2016) correlate well with observations of 4-5-m diameter full scale unsupported tunnels excavated within a highly silicified rock mass. In this example the rock has a Uniaxial Compressive Strength of 250-270 MPa and widely spaced, tightly healed geological discontinuities. The onset of stress driven failure in these full scale unsupported tunnels was experienced where the ratio of intact rock strength to maximum induced tangential stress was

approximately 3.5. The mining tunnels were constructed using excellent drilling and blasting techniques. The tunnels were designed with semi-circular walls and a flat floor. Incipient failure of the tunnel back (roof) due to a sub-horizontally oriented major principal stress component can be seen in Fig. 6.



Fig. 6. Full scale unsupported semi-circular tunnels showing the on-set of brittle spalling failure at the centre of the excavation roof due to high horizontal stress.

## 2.2 Structurally Controlled Shear Failure

Testing of scaled-down tunnels by Kusui (2016) has shown that under progressively increased loading conditions, the initial spalling failure is followed by shear failure of the walls adjacent to the tunnel geometry. Fig. 7 shows the load-displacement profile and acoustic emission count for an example of such progressive brittle failure of a tunnel under increased loading. After spalling, large shear cracks can propagate adjacent to the tunnel with shear failure dominating the latest stages of the failure mechanism. The results show the seismic response in which loading was gradually increased from zero until tunnel wall spalling and pillar crushing were sequentially experienced. The seismic activity starts with the creation of a vertical tension crack in the floor and roof of the circular opening, as predicted by theory (Hoek & Brown, 1980). The rate of seismic activity clearly increased prior to the violent ejection in both walls. Significantly, relatively few acoustic emissions were monitored during the period between spalling and the onset of the shear failure mode of pillar crushing. Overall, a significant decrease in load bearing capacity occurs following the final shear mode of failure.

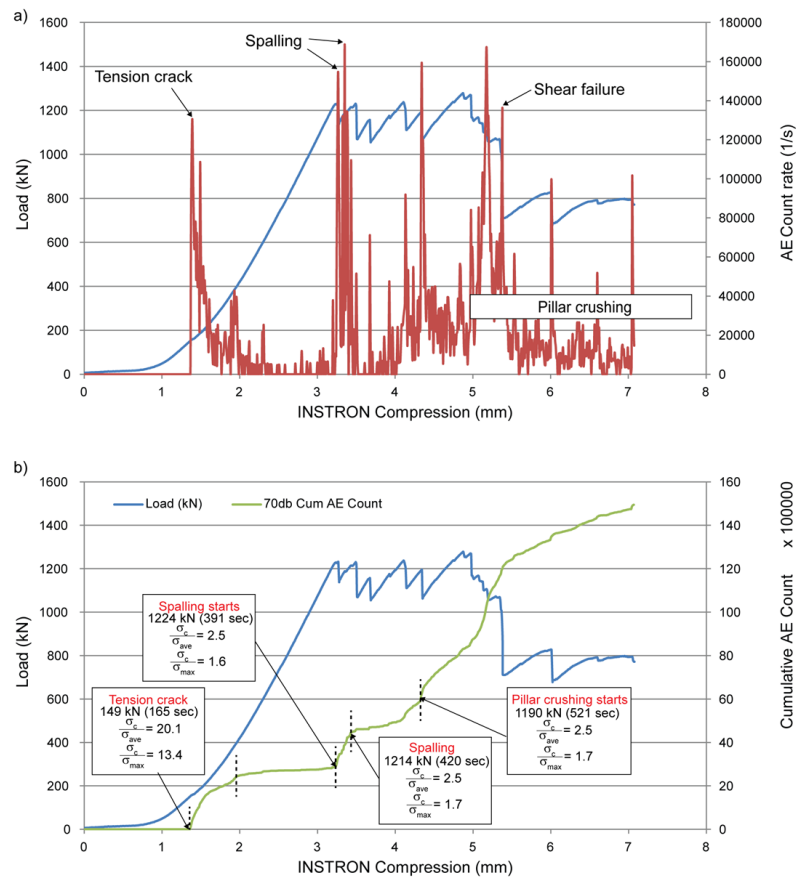


Fig. 7. Failure mode, rate of seismicity and decreasing ratios of strength/induced stress for an unsupported tunnel in strong sandstone (Kusui, 2016).

### 2.3 Damage and Deformation Prior to Violent Failure

The on-set of tunnel damage and progression to violent failure in massive rock has been studied in detail by Kusui et al (2016). As shown above, the complete excavation response has been determined as the induced stress near the excavation boundary is increased with respect to the intact rock strength. The critical levels of strength to induced stress related to the onset of visible instability such as spalling on both walls and the start of pillar crushing were calculated. The results show that the failure threshold values of  $\sigma_c/\sigma_{max}$  are dependent upon the Uniaxial Compressive Strength. Higher values of  $\sigma_c/\sigma_{max}$  at failure correlate to lower radial strain at failure (Fig. 8). This is in accordance with field data reported by Hoek (1999) and laboratory work on critical strain by Li (2004).

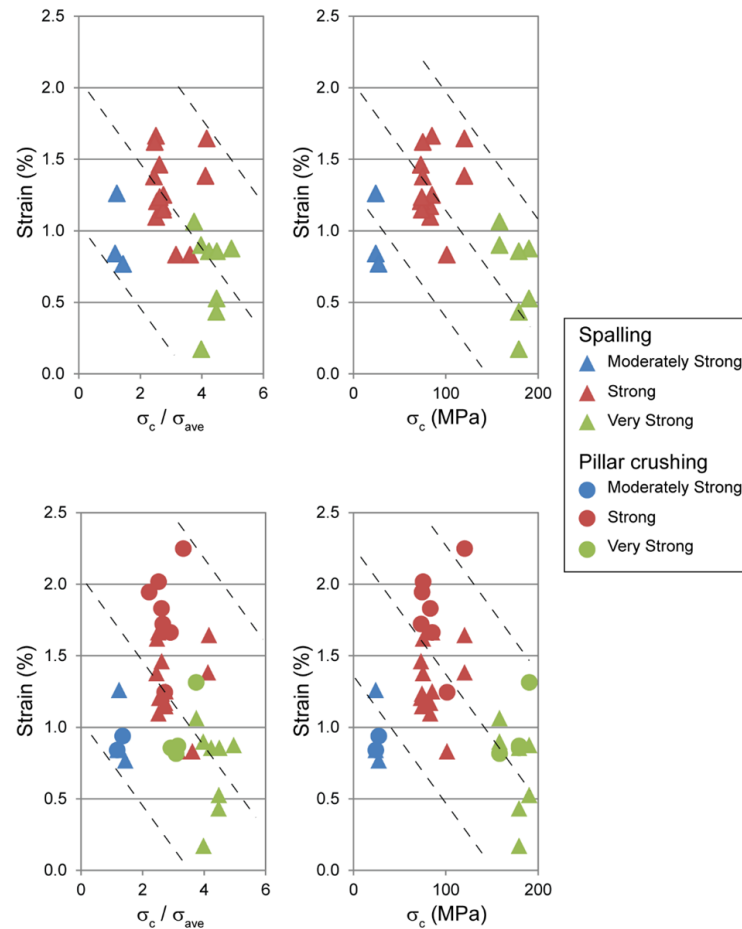


Fig. 8. Higher strength materials exhibit lower radial strain at failure (Kusui et al, 2016).

### 3. Ejection Velocity

For tunnels constructed in very strong rock, violent ejection occurs simultaneously with crack propagation along the tunnel axis. The crack propagation is perpendicular to the orientation of the main principal stress component. Once slabs are detached from the tunnel surface, they are ejected violently with associated rock failure noise. Laboratory testing by Kusui (2016) has established ejection velocities ranging from 3 - 10 m/sec across a variety of rock types, which validates back analysis of actual failures in underground mining (Ortlepp, 1993). A typical result for a wall failure is shown in Fig. 9, where an ejection velocity of 5.2 m/sec can be determined using a background grid. Similar velocities have been used at the WA School of Mines during dynamic testing of rock reinforcement systems (Villaescusa et al., 2010). Such ejection velocities are capable of damaging most commercially available ground support schemes.

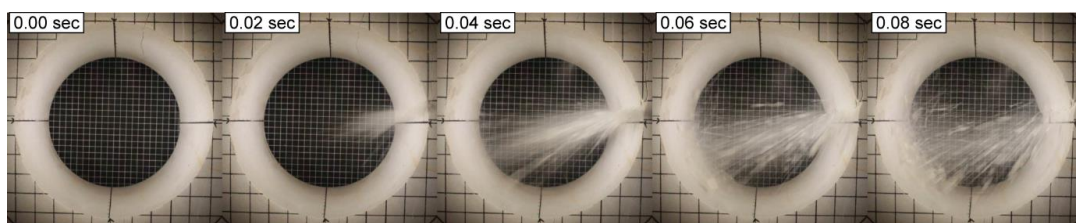


Fig. 9. Determination of ejection velocity using a high speed video camera.

Kusui (2016) calculated average ejection velocities of 200 mm diameter unsupported tunnels as a function of the Uniaxial Compressive Strength. Ejection velocities ranging from 2-10 m/sec were determined, which validated the back analysis of actual failures in underground mining (Ortlepp & Stacey, 1994, Drover & Villaescusa, 2015). Generally, the higher the UCS, the higher the measured ejection velocity. Such positive correlation between the intact rock strength and the velocity of ejection is consistent with the tunnel observations of Broch and Sørheim (1984). Kusui (2016) also tested scaled-down tunnels which were stabilized using a number of ground support schemes (Kusui & Villaescusa, 2016). Fig. 10 compares the average ejection velocity results for unsupported and supported tunnels. The results show that the ejection velocity is reduced when a surface support system is installed. The results also show that the reinforcement element installation pattern also influences the ejection velocity, with staggered patterns proving to be more effective than square patterns of the same reinforcement scheme and spacing. The ejection velocity results for staggered patterns of 2.6 m/s and 4.4 m/s are in the low range of the measured values. Additionally, when a mesh layer was installed, the ejection velocity was lower than when shotcrete was exposed as the final layer. Shotcrete ejection velocities determined in the laboratory experiments were similar to those calculated from back analysis of full scale tunnel conditions (Fig. 11).

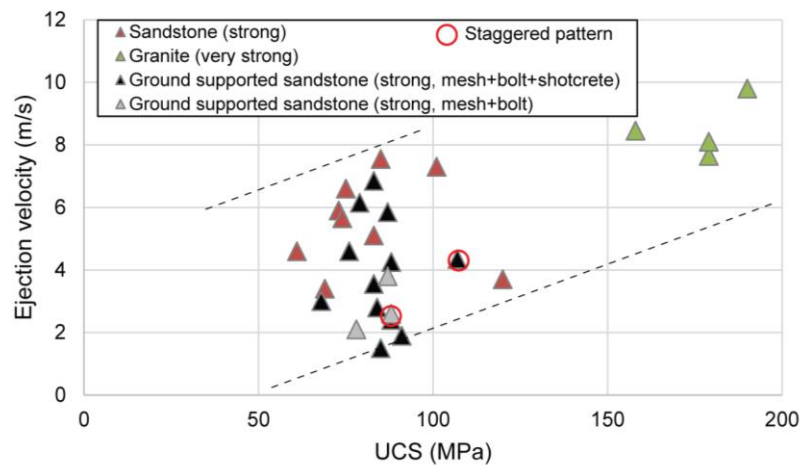


Fig. 10. Ejection velocity as a function of UCS for unsupported and stabilized tunnels (Kusui, 2016).



Fig. 11. Example of violent spalling through a shotcrete layer exposing the rock surface.

#### 4. Ground Support Demand

Ground support design is often based on previous experience from similar geotechnical environments and work practices. Challenging this approach is the fact that the rock mass conditions usually change with the progress of a mine and the ground support performance may become unacceptable over time. That is, when the induced stresses increase due to greater depth of mining or global extraction increases, the installed reinforcement and support capacities may not satisfy the rock mass demand. Geological models of rock strength variability, in-situ stress measurement data and 3D non-linear numerical stress modelling may be used to investigate potential changes in excavation loading conditions ahead of the development horizons. Routine collection and analysis of such data is necessary for continuous ground support design verification throughout the mine life.

The generic procedure for ground support design consists of several distinct steps (Thompson et al, 2012):

1. Identify a mechanism of failure.
2. Estimate the areal support demand.
3. Estimate the reinforcement length, force and displacement demand.
4. Estimate the energy demand of the complete scheme.
5. Select appropriate reinforcement and support systems.
6. Propose arrangement of reinforcement and support systems and evaluate.
7. Specify the complete ground support scheme.

This procedure may need to be applied to several different observed mechanisms and depths of failure, which in turn control the ground support demand. In general, the energy demand from a particular failure is controlled by the amount of mass that becomes unstable and the velocity of its ejection. The unstable mass can be expressed in  $T/m^2$ , reflecting the maximum mass in tonnes of unstable rock that was ejected per unit area of the excavation surface where failure occurred. For the purposes of design, demand may be quantified in terms of the kinetic energy of the ejected rock. This design approach considers that strain energy released by the rock mass during violent stress-driven failure is partially converted into kinetic energy of ejected blocks. These blocks load the ground support scheme dynamically, causing a force-displacement response. The mass of unstable rock that is violently ejected and the initial velocity of its ejection are the critical input variables in the kinetic energy calculation.

The mass of instability may be quantified via probabilistic analysis of the local structural geological data. For structurally controlled mechanisms of failure, it may be reasonably assumed that the unstable mass is controlled by the largest possible tetrahedral wedge able to be formed by the prevailing structural conditions. For pure spalling mechanisms, observational experience indicates that the mass of instability is limited by a depth of failure of 0.5 metres or so in moderately strong rock. The spalling depth of failure progressively decreases with increasing rock strength.

The initial velocity of rock ejection may be estimated most reliably from the Uniaxial Compressive Strength of the excavation host rock. Kusui, 2015, recently demonstrated the dependence of ejection velocity on intact rock UCS via a series of scaled-down laboratory tests of circular excavations in hardrock. These experiments revealed an approximately linear relationship between UCS and ejection velocity, from which a first degree polynomial trend line equation was derived. Considering this relationship, plotting of the kinetic energy equation solutions for a range of rock types and instability scenarios yields the chart in Fig. 12. This figure shows the estimated kinetic energy demand on a ground support scheme imposed by a range of unstable masses, as a function of the ejection velocity. This demand chart has been calibrated with back analysis of actual violent failures occurring in a range of material strengths. It may also be used as a design tool to estimate energy demand on a ground support scheme, considering the potential modes of failure and site-specific mechanical characteristics of the rock mass.

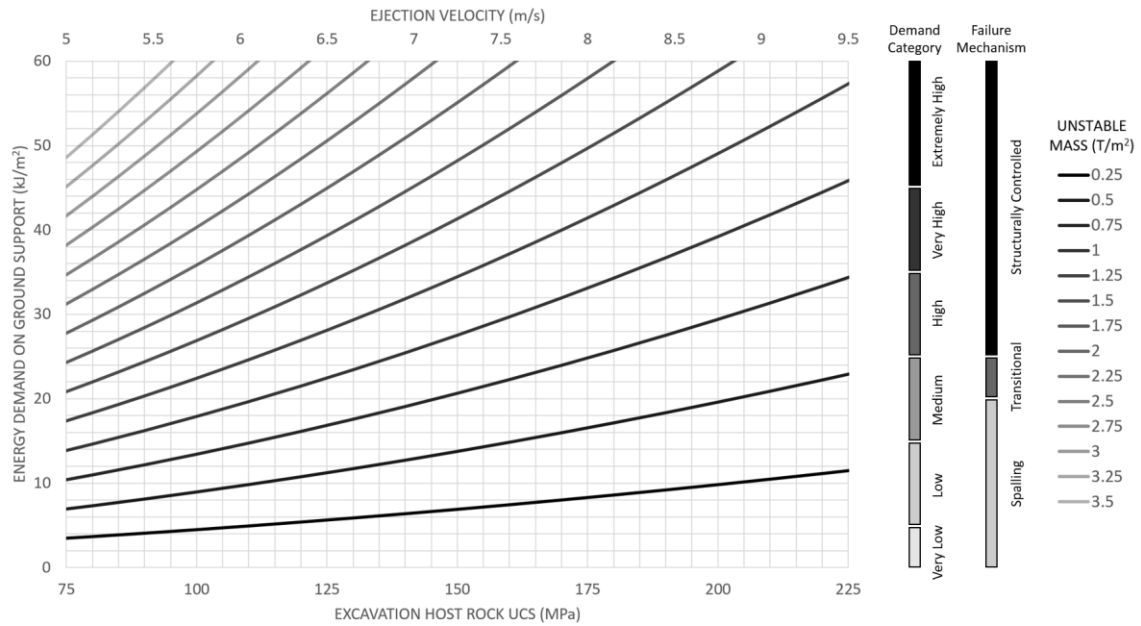


Fig. 12. Range of energy demand on ground support for stress-driven failures in hard rock.

#### 4.1 Shallow Depth of Failure (Spalling)

For the majority of the rock masses experiencing seismicity and related dynamic ejections, the depth of failure is shallow, with instability often limited to a depth range of 0.25 - 0.5 m or so (Fig. 13). This spalling mechanism of failure is likely to preferentially load the surface support, including shotcrete and mesh layers, as well as rockbolt and cablebolt plates. The mass of instability associated with spalling style failure ranges from approximately 0.6 to 1.3 T/m<sup>2</sup> in the majority of hard rocks. This would most likely test the surface retention capacity of the chosen ground support scheme. In terms of energy demand, for a range of hard rock conditions, spalling failure mechanisms could be expected to generate up to 20kJ/m<sup>2</sup> demand on the ground support scheme. Energy demand above this threshold is more likely to be structurally controlled.



Fig. 13. Example of violent, but shallow depth of failure preferentially loading the bolt-plate interface causing failure at less than 5 kJ/m<sup>2</sup>.

#### 4.2 Structurally Controlled Failure

In cases where violently mobilised geological structures approach the span width of an excavation, the depth of failure may be very large, sometimes exceeding 2.0 metres. Such instability can occur due to rupture along major structures, which in some cases intersect the excavation boundaries where reinforcement and support has been installed. The presence of geological structures continuous on the scale of the tunnel walls increases the depth of failure. The observed damage frequently consists of shear failure along structures, resulting in a sudden and violent ejection of large blocks. Because of the large depth of failure, it is likely that the ejection will damage a large number of reinforcement elements, followed by the destruction of the surface support layers (Fig. 14). Structurally controlled violent failure is expected to result in the mass of instability exceeding 1.5 T/m<sup>2</sup> with energy dissipation often well in excess of 25 kJ/m<sup>2</sup>. In some difficult conditions, the energy demand could locally exceed 60-80 kJ/m<sup>2</sup> (Drover and Villaescusa, 2015).



Fig. 14. Example of violent and structurally controlled failure that has broken reinforcement elements and ruptured the surface support layers.

Geotechnical mapping and underground observations are required to determine if large scale instability may be developing within the unsupported spans that are exposed immediately after development blasting and prior to the installation of ground support layers, such as in-cycle shotcrete. Information from structural geotechnical mapping can be used as an input for probabilistic determination of large scale instability, considering all possible wedge geometries likely to become unstable (Fig. 15). This information can be used to design the length of high energy dissipation reinforcement elements, such as cement grouted and plated twin strand plain cablebolts. These may also be installed with two layers of high strength woven steel mesh (Kusui and Villaescusa, 2016).

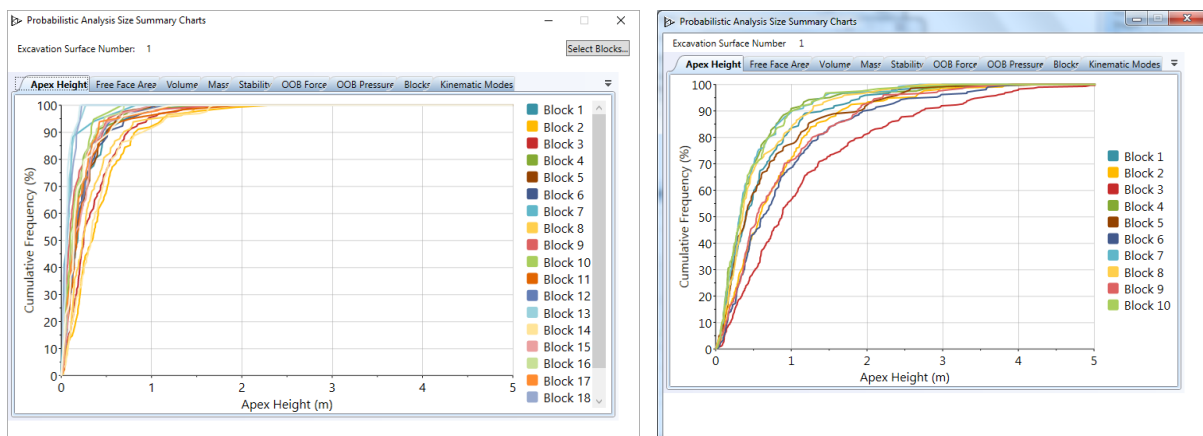


Fig. 15. Example of summary of probabilistic stability results for potentially unstable apex heights for tetrahedral block shapes for two mine sites.

## 5. Ground Support Capacity

The required force-displacement response and energy dissipation capacity of a ground support scheme should exceed the rock mass demand imposed upon the excavation. Depending upon the depth of failure, this rock mass demand may be applied directly from the rock mass or through the support membrane that is retained by the reinforcement elements. Villaescusa et al (2014) have defined rock mass demand in terms of ranges of allowable displacement and energy (Table 1) and combined it with the WA School of Mines dynamic reinforcement capacity database (Player, 2012). Example design charts for rock reinforcement only and combined reinforcement and mesh schemes tested under

dynamic loading are shown in Fig. 16 and Fig. 17 respectively. For each rock mass demand category, the corresponding ranges of displacement and energy were used to define a region, shown as a box, that has been labelled very low, low, medium, high, very high and extremely high energy demand. For each region, the acceptable ground support scheme components should have similar displacement compatibility, while providing higher energy dissipation capacity than the required demand. That is, for each demand region, the recommended reinforcement would plot within the green design region.

Table 1. Typical rock mass demand for ground support design (Modified after Villaescusa et al. 2014).

Demand category	Reaction pressure (KPa)	Surface displacement (mm)	Energy (KJ/m <sup>2</sup> )
Very Low	<100	<50	<5
Low	100-150	50-100	5-15
Medium	150-200	100-200	15-25
High	200-400	200-300	25-35
Very High	400-500	300-400	35-45
Extremely High	>500	>400	>45

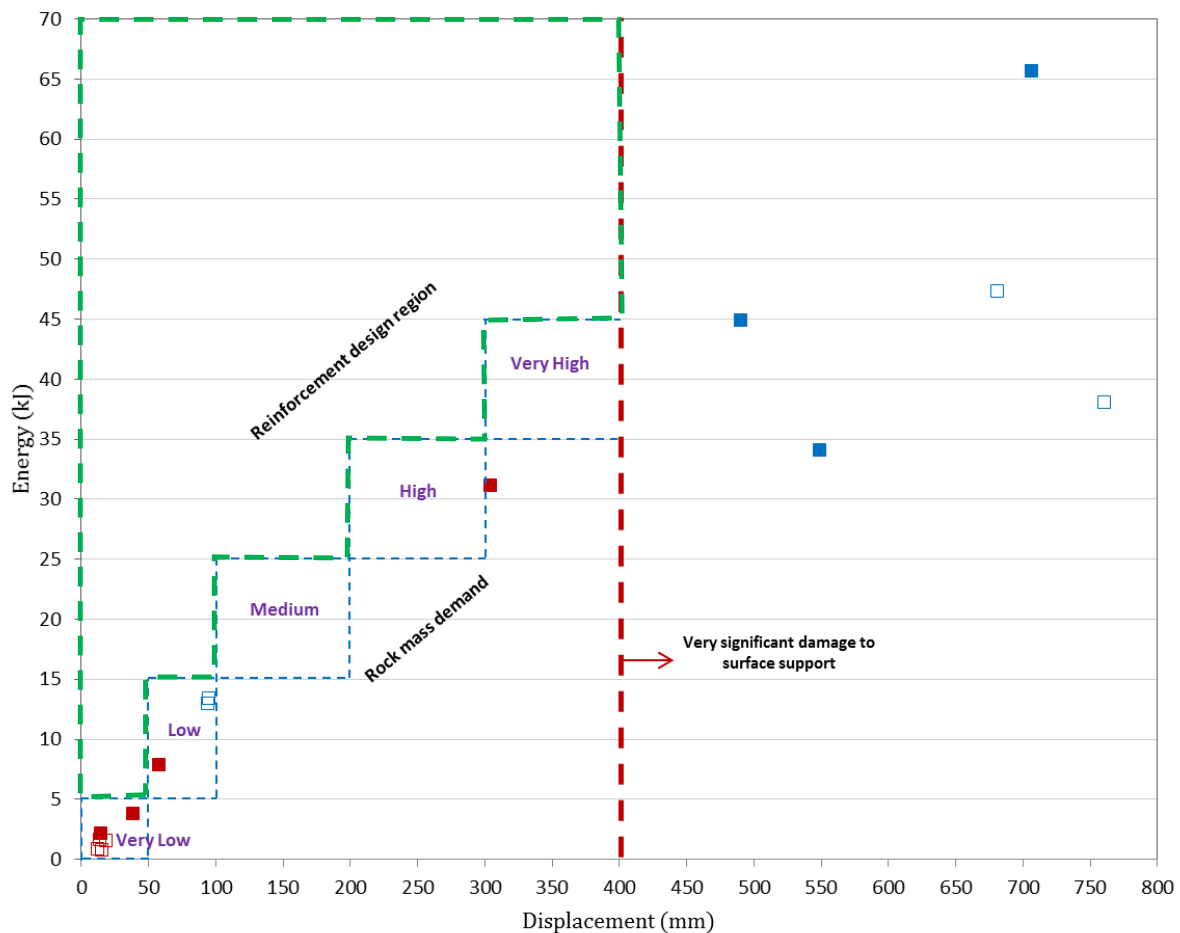


Fig. 16. Dynamic energy dissipation versus displacement at failure for CFC reinforcement elements tested at WA School of Mines Dynamic Test Facility.

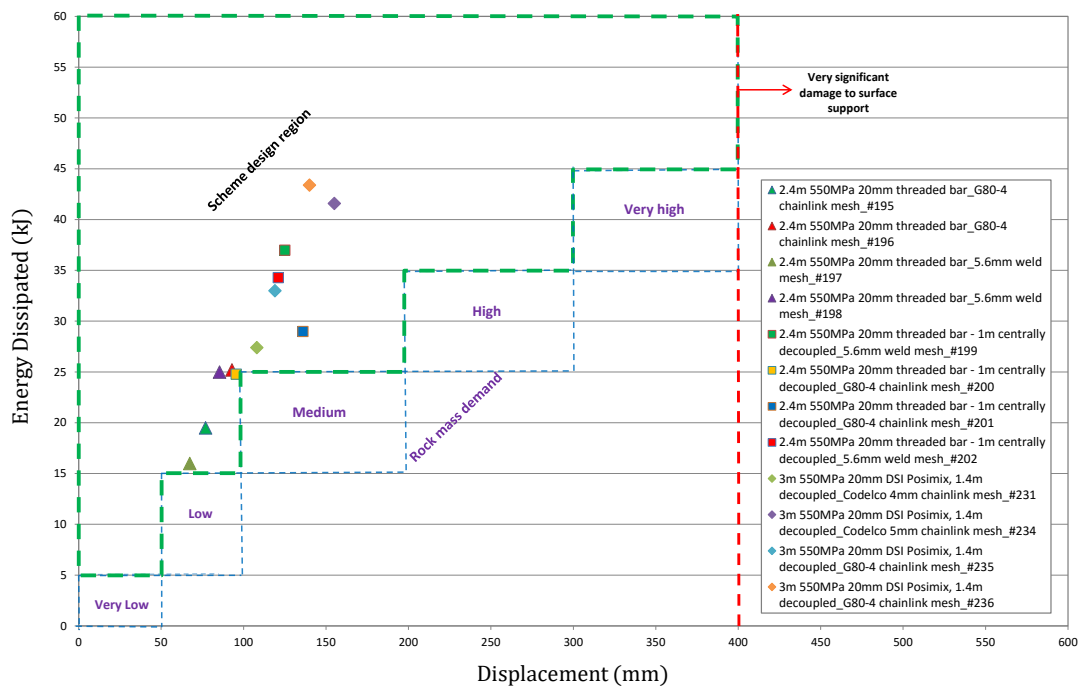


Fig. 17. Dynamic energy dissipation versus displacement at failure for combined schemes of rock bolts and mesh tested at WASM (Villaescusa et al, 2016).

## 6. Ground Support Design for Extremely High Demand Conditions

In future years, as the depth of mining and tunnelling operations generally increases worldwide, energy demand conditions exceeding  $45\text{kJ/m}^2$  can be expected to be encountered more frequently. During the development stage of a project, leading tunnels can enter conditions of extreme energy demand. Failure at this stage of the project can lead to significant schedule impacts, costing millions of dollars in lost revenue or rehabilitation expenditure. Similarly, large failures occurring during the production phase of a mine or service phase of a civil excavation can also result in loss of revenue. Already a small number of mining operations have experienced failure mechanisms which generated in excess of  $60\text{--}80\text{kJ/m}^2$  sudden and violent energy demand on the ground support scheme (Drover & Villaescusa, 2015a). This level of demand may be very highly localized to an area of no more than 5-10 square metres of the excavation surface, for example where rupture of a significant geological structure coincides with an excavation. Nonetheless, severe ground support scheme damage can occur as a result. As such, in order to ensure continuity of tunnelling operations at great depth, it is necessary to formulate a ground support scheme arrangement which can adequately manage this level of energy demand.

Laboratory experiments at WASM and field observations of extremely high energy demand failure events at several mines indicate that the superior ground support scheme arrangement includes a multi-layered, integrated scheme of very high energy dissipation capacity components. The first stage of a ground support scheme for extremely high energy dissipation includes a primary shotcrete layer of approximately 75mm thickness, internally reinforced with high tensile (1770MPa) woven steel mesh. Woven steel mesh is preferred due to the fact that its energy dissipation capacity significantly exceeds that of common variety mild steel weld mesh (Villaescusa et al. 2012). The ability of high tensile woven mesh to articulate post-fracture of the shotcrete, as well as its superior stiffness and displacement performance under load also support its selection for extreme demand conditions. Fibres are not required to be included in shotcrete that is internally reinforced with woven mesh in this context, due to the relatively negligible strength performance benefit that fibres provide under extreme loading, both pre and post-fracture (Drover & Villaescusa, 2015a). A 75mm thick, internally mesh reinforced

shotcrete layer of this construction can be expected to dissipate approximately 15-20 kJ/m<sup>2</sup> of energy demand if using, for example, a 4mm wire diameter, 80mm aperture woven mesh product with 30-35 MPa (28 day) strength shotcrete.

This surface support system can be installed in conjunction with a primary reinforcement pattern, utilising 25mm diameter, cement encapsulated (fully grouted) 550MPa threaded rebar in a continuously mechanically coupled (CMC) arrangement. WASM testing data (Villaescusa et al, 2014) indicate that these elements are capable of dissipating up to 45 kJ dynamically. A 1m x 1m staggered pattern spacing of the reinforcement elements is standard, but this spacing may be optimized, depending on the demand estimated from probabilistic structural analysis of potentially unstable wedges. The benefit of the staggered pattern is its ability to arrest and contain fracture propagation within a bolt spacing. This prevents fractures from extending over multiple bolt spacings, with associated increased displacements, as would be observed for a square pattern (Fig. 18). This first pass of surface support and reinforcement constitutes the primary ground support scheme sequence.

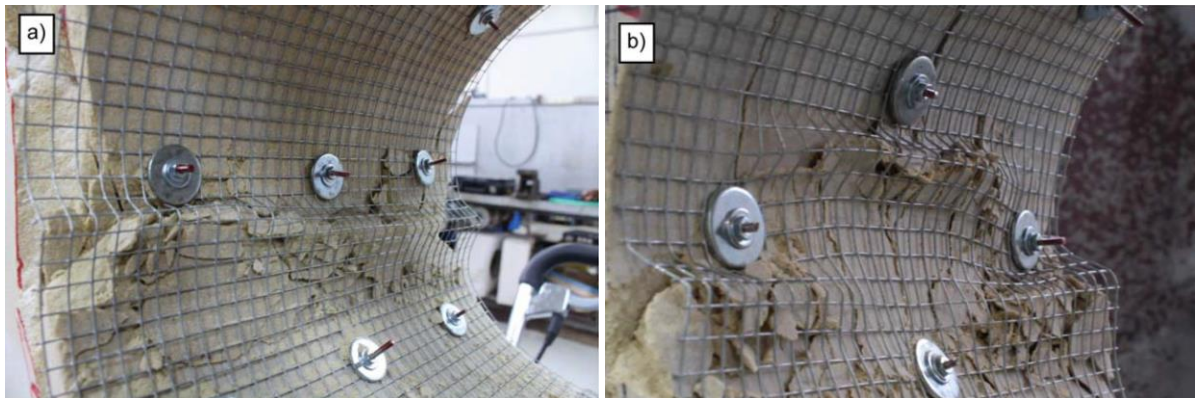


Fig. 18. Square (a) versus Staggered (b) reinforcement pattern performance during failure (Kusui, 2016).

In conditions of extremely high energy demand, it is typically necessary to install an overlapping secondary ground support scheme sequence. This secondary layer provides additional energy dissipation capacity and surface support redundancy connected to deep reinforcement. The secondary layer of woven mesh surface support is installed externally to the primary surface support layer and is connected to deep reinforcement in the form of twin plain strand cable bolts of approximately 5-7m length. Cables are positioned also on a staggered 1m x 1m pattern, spaced evenly in between the primary threaded bars (Fig. 19). In the event that structurally controlled failures with large blocks overload the primary reinforcement and surface support layer, this secondary layer provides load transfer connectivity from the unstable to stable regions of the excavation via the external mesh (Fig. 20). Deep reinforcement assists to anchor the unstable material to solid stable ground. An external layer of high tensile woven mesh with 5mm wire diameter and 80mm aperture can be expected to dissipate up to 25 kJ/m<sup>2</sup> dynamically, whereas twin strand cables may dissipate a combined 40kJ under dynamic loading. The complete ground support scheme arrangement is illustrated in Fig. 19. For deep failures which initially mobilize reinforcement, this scheme can be expected to dissipate in excess of 60 kJ/m<sup>2</sup> under extremely high demand conditions.

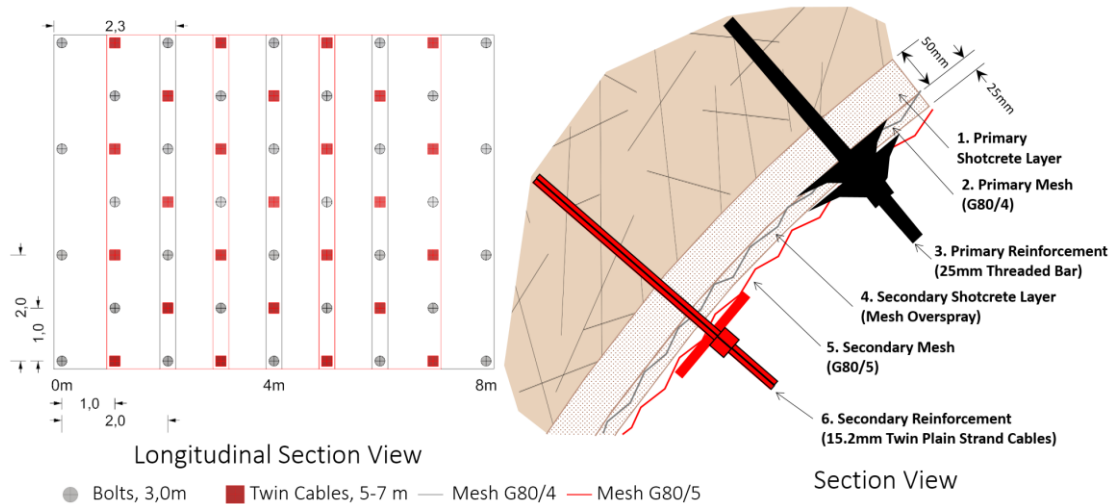


Fig. 19. Example of a multi-layered, integrated ground support scheme for extremely high energy dissipation capacity.



Fig. 20. An external layer of high capacity woven mesh surface support connected to secondary deep reinforcement provides load transfer from the unstable to stable regions of an excavation.

## 6. Conclusions

Back analysis of actual failures in underground mining indicate that the higher the material strength, the higher the measured ejection velocity. Similar results have been determined from scaled-down tunnel experiments, which have been used to establish a range of solutions for kinetic energy of ejection, considering the potential instability scenarios of a range of rock types. In cases where the depth of failure is shallow, with instability often limited to a depth range of 0.25 - 0.5 m or so, this would most likely test the surface retention capacity of the chosen ground support scheme. In terms of energy demand, for a range of hard rock conditions, spalling failure mechanisms could be expected to generate up to 20 kJ/m<sup>2</sup> demand on the ground support scheme. In cases where the depth of failure is large (i.e., exceeding 1 to 2m), this usually involves the mobilisation of geological structures. The observed damage frequently consists of shear failure along structures, resulting in a sudden and violent ejection of large blocks. Because of the large depth of failure, it is likely that the ejection will damage a large number of reinforcement elements, followed by the destruction of the surface support layers. Structurally controlled violent failure is expected to result in the mass of instability exceeding 1.5 T/m<sup>2</sup> with energy dissipation often well in excess of 25 kJ/m<sup>2</sup>. For such cases a multi-layered, integrated ground support scheme capable of extremely high energy dissipation capacity is recommended.

## Acknowledgements

The writers wish to acknowledge the WA School of Mines/Curtin University, CRC Mining, and the many other supporting organisations, including mining companies and ground support product suppliers. The contributions of many colleagues at the WASM Rock Mechanics Group are also gratefully acknowledged.

## References

- Barla, G., 2014. TBM tunnelling in deep underground excavation in hard rock with spalling behaviour. Proceedings of the 43rd Geomechanics Colloquium, 25-39.
- Barton, N., Lien, R. & Lunde, J., 1974. Engineering classification of rock masses for design of tunnel support. *Rock Mechanics*, 6(4), pp. 189-236.
- Broch, E., & Sørheim, S., 1984. Experiences from the planning, construction and supporting of a road tunnel subjected to heavy rockbursting. *Rock Mechanics and Rock Engineering*, 17(1), 15-35. doi: 10.1007/BF01088368.
- Christiansson, R., Hakala, M., Kemppainen, K., Siren, T., & Martin, C. D., 2012. Findings from Large Scale In-situ Experiments to Establish the Initiation of Spalling. Paper presented at the ISRM International Symposium-EUROCK 2012, Stockholm, Sweden.
- Diederichs, M. S., 2007. The 2003 Canadian Geotechnical Colloquium: Mechanistic interpretation and practical application of damage and spalling prediction criteria for deep tunnelling. *Canadian Geotechnical Journal*, 44(9), 1082-1116.
- Drover, C. & Villaescusa, E., 2015a. Estimation of dynamic load demand on a ground support scheme due to a large structurally controlled violent failure - a case study. *Journal of Mining Technology*, 125(4).
- Drover, C. & Villaescusa, E., 2015b. Performance of shotcrete surface support following dynamic loading of mining excavations. Proceedings of Shotcrete for Underground Support XII, Singapore.
- Hoek, E. & Brown, E., 1980. *Underground Excavations in Rock*. London, UK: IMM.
- Hoek, E., 1999. Support for very weak rock associated with faults and shear zones. In E. Villaescusa, C. R. Windsor & A. G. Thompson (Eds.), *Rock Support & Reinforcement Practice in Mining* (pp. 19-32). Rotterdam: Balkema.
- Hutchinson, D. & Diederichs, M., 1996. *Cablebolting in Underground Mines*. 406pp. Richmond, British Columbia, Canada: Bitech Publishers.
- Kusui, A., 2016. Scaled down tunnel testing for comparison of surface support performance, PhD Thesis, WA School of Mines, Curtin University: Kalgoorlie, Western Australia, 216p.
- Kusui, A., Villaescusa, E. & Funatsu, T., 2016. Mechanical behaviour of scaled-down unsupported tunnel walls in hard rock under high stress, *Tunnelling and Underground Space Technology* 60:30-40.
- Kusui, A. & Villaescusa E., 2016. Seismic Response Prior to Spalling Failure in Highly Stressed Underground Tunnels, Proc. Seventh International Conference & Exhibition on Mass Mining 2016, The AusIMM, Sydney, Australia.
- Lajtai, E., & Dzik, E., 1996. Searching for the damage threshold in intact rock. *Rock Mechanics: Tools and Techniques*, Aubertin, Hassani & Mitri (eds.), Balkema, 1, 701-708.
- Li, J. 2004. Critical Strain of Intact Rock and Rock Masses. Ph.D. Thesis, Curtin University of Technology, 186p.
- Martin, C. D., 1993. The strength of massive Lac du Bonnet granite around underground openings. PhD Thesis, University of Manitoba Manitoba, Canada.
- Martin, C. D., 1997. Seventeenth Canadian Geotechnical Colloquium: The effect of cohesion loss and stress path on brittle rock strength. *Canadian Geotechnical Journal*, 34(5), 698-725.
- Mathews, K. E., Hoek, E., Wyllie, D. C., & Stewart, S. B. V., 1980. *Prediction of Stable Excavation Spans for Mining at Depths Below 1,000 Meters in Hard Rock*. Ottawa, Ontario, Canada: Golder Associates Report to Canada Centre for Mining and Energy Technology (CANMET), Department of Energy and Resources.
- Ortlepp, W. D., 1993. High Ground Displacement Velocities Associated with Rockburst Damage. *Rockbursts and Seismicity in Mines* 93, 101-106.
- Ortlepp, W. D., & Stacey, T. R., 1994. Rockburst mechanisms in tunnels and shafts. *Tunnelling and Underground Space Technology*, 9(1), 59-65. DOI: [http://dx.doi.org/10.1016/0886-7798\(94\)90010-8](http://dx.doi.org/10.1016/0886-7798(94)90010-8)

Player, J., 2012. Dynamic Testing of Rock Reinforcement Systems, PhD Thesis: Western Australian School of Mines, Curtin University of Technology, Perth, Western Australia, Australia, 501p.

Thompson, A. & Windsor, C., 1992. A classification system for reinforcement and its use in design. Proceedings of the Western Australian Conference on Mining Geomechanics, Kalgoorlie, Western Australia, Australia, Western Australian School of Mines, pp. 115-125.

Thompson, A., Villaescusa, E. & Windsor, C., 2012. Ground Support Terminology and Classification - An Update. *Geotechnical and Geological Engineering*, 30(3), pp. 553-580.

Villaescusa, E., Thompson, A. G., Player, J. R., & Morton, E. C., 2010. Dynamic Testing of Ground Control Systems. Report No. 287, 187p: Minerals and Energy Research Institute of Western Australia.

Villaescusa, E. et al., 2012. A Database of Static and Dynamic Energy Absorption of Mesh for Rock Support. Proceedings of the 2012 Australian Mining Technology Conference, Perth, Western Australia, Australia 8-10 October, pp.27-34.

Villaescusa, E., Player, J. R., & Thompson, A. G., 2014. A Reinforcement Design Methodology for Highly Stressed Rock Masses, 8th Asian Rock Mechanics Symposium, DOI: 10.13140/2.1.4423.8402.

Villaescusa, E., 2014. Geotechnical design for sublevel open stoping. CRC Press, 519p.

Villaescusa, E, U. de Zoysa, J.R. Player & A.G. Thompson, 2016. Dynamic Testing of Combined Rock Bolt and Mesh Schemes, Procc. Seventh International Conference & Exhibition on Mass Mining 2016, The AusIMM, Sydney, Australia.